POAC'25
St. John's, Newfoundland and Labrador, Canada

Proceedings of the 28th International Conference on Port and Ocean Engineering under Arctic Conditions
Jul 13-17, 2025
St. John's, Newfoundland and Labrador
Canada

Wind-Ice Interaction Under Variable Wind Velocities: Integration of Particle Image Velocimetry (PIV) and Particle Tracking Velocimetry (PTV)

Parisa Radan[1], Wojciech Artichowicz[1], Maciej Paprota[2] and Tomasz Kolerski[1*]
[1] Gdansk University of Technology, Gdansk, Poland
[2] Institute of Hydro-Engineering, Polish Academy of Science, Gdansk Poland

ABSTRACT

The study investigated wind-ice interactions under stationary water conditions using the wave flume at the Institute of Hydro-Engineering, Polish Academy of Sciences (IBW PAN). Key parameters included ice concentration, ice size, and wind velocity. Non-thermal ice simulation was achieved using polypropylene cut pellets. A wind tunnel positioned above the water surface was used for generation of three distinct wind velocity fields representing low, medium, and high wind velocities. Wind velocities were measured using the Particle Image Velocimetry (PIV) technique with water mist as the seeding material, marking its first application for wind velocity ranges of 0.5 to 1.5 m/s. Ice velocity was determined using Particle Tracking Velocimetry (PTV), with the ice itself serving as the tracer. Experimental results were compared with the DynaRICE model. Findings indicated that as wind velocity increased, the wind-drag coefficient decreased (ranging from 0.009 to 0.002). The default wind-drag coefficient value of 0.0015, used in the DynaRICE model, was deemed appropriate for simulations conducted in higher wind velocity ranges relative to this study.

KEY WORDS Wind drag; Ice drift; Numerical modeling

INTRODUCTION

Wind is one of the main factors influencing the movement of surface ice in water bodies where the water flow velocity is low. This applies to lakes (Kolerski et al., 2013), large reservoirs (Kolerski, 2021), as well as lagoons such as the Vistula Lagoon (Kolerski et al., 2019, Kolerski et al. 2023). Wind can also directly cause ice movement, causing acceleration, directing it towards one of the shores, or completely halting its outflow (Majewski, 2011). These phenomena affect both ice dynamics and generate loads when the ice comes into contact with the shoreline, embankments, or structures (Hammer et al., 2023).

The transfer of wind force to ice has been studied, primarily focused on wind effects on sea ice

in the Arctic (Guest and Davidson, 1991; Overland, 1985). The most widely used approach is the formula proposed by (Wu, 1973a), in which ice velocity is determined as a function of wind speed through a correction coefficient. This coefficient is assumed to be constant and independent of ice parameters.

In this study, we aimed to determine the influence of ice parameters, such as the size of individual ice pieces and ice concentration, on its velocity when driven solely by wind. To achieve this, we conducted medium-scale experiments in a hydraulic laboratory and numerical simulations using the DynaRICE model.

METHODOLOGY

The research was conducted at the Institute of Hydro-Engineering, Polish Academy of Sciences in Gdansk-Oliwa. The experiments were carried out in a wave flume, which was adapted for the specific study. A low-cost aerodynamic tunnel was constructed using simple materials such as plywood and plexiglass. Wind was generated by three fans, which were activated sequentially—using one, two, or all three at a time. Figure 1(a) Depicts the laboratory flume setup, modified with an aerodynamic tunnel and a plexiglass-covered measurement section.

Velocity measurements were recorded using a Particle Image Velocimetry (PIV) system, which enabled the measurement of both air and water velocities. For water velocity measurement, glass spheres were introduced into the water. For air velocity measurement, different tracers were tested, including smoke, water vapor, and water mist. After analysis, water mist was determined to be the most suitable tracer for the experiment. This decision was based on the fact that water mist is non-aggressive, does not interact with the instruments, and does not contribute to water contamination. Additionally, PIV-based tests confirmed that the spatial distribution of water mist in the air yielded satisfactory results and allowed for reliable velocity measurements. Figure 1(b) Shows the use of Particle Image Velocimetry (PIV) to measure wind speed within the setup.

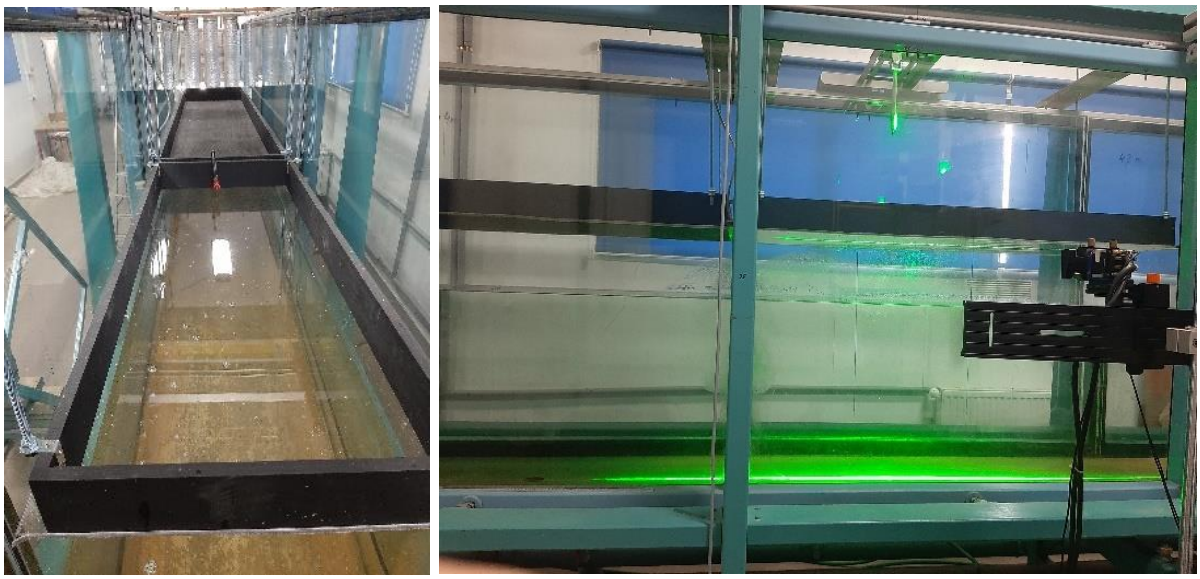

Figure 1. The laboratory channel with an added aerodynamic tunnel, including a measurement

section covered with a plexiglass sheet (a), and wind speed measurement using the PIV methodology (b).

To verify the accuracy of the PIV measurements, an independent invasive measurement was conducted using an Omni Instruments micro-velocimeter with a 0.5 cm propeller diameter. A comparison between the invasive method (propeller-type velocimeter) and the non-invasive PIV method showed a high level of agreement.

The next part of the experiment focused on measuring ice velocity using the Particle Tracking Velocimetry (PTV) technique. Since the hydraulic laboratory did not allow for controlled temperature testing, real ice was not used. Instead, a substitute material with ice-like properties was tested. Various materials were considered, and polypropylene (PP) sheets were ultimately selected, as they have the same density as freshwater ice (917 kg/m³), are relatively inexpensive, readily available, and easy to process.

These PP sheets were used to create repeatable ice-like elements with:

- Small fragments (10 × 10 cm, 1 cm thick) to simulate broken ice formed during ice movement.
- Larger slabs (0.5 m × 0.6 m, 1 cm thick) to simulate ice cover fragments that had broken but remained as single floating sheets.

The aim of this experiment was to analyze the wind's impact on ice dynamics. The tests were conducted without water flow, isolating the effect of wind on ice transport.

A series of experiments were performed under varying wind speeds and ice sizes:

- Small and large ice plates were tested.
- Different ice concentrations were introduced: low, medium, and high concentrations, where the latter was close to full ice coverage of the channel.
- Three wind speeds were used, corresponding to the activation of one, two, or three fans.

Experiments with large ice slabs were conducted under only one set of conditions. The results included measured ice velocity under different input parameters. Due to time constraints, only the described series of experiments were conducted, but each experiment was repeated multiple times (two to three repetitions) for reliability.

The final phase of the experiment involved comparing the PTV measurement results with numerical simulations using the DynaRICE mathematical model (Liu and Shen, 2005). The PTV computations are done with PTVlab Software (Brevis et al., 2011). The model was directly adapted to the experimental setup, meaning no scaling was applied, and the same geometric dimensions were used in the numerical model.

The numerical simulations were designed to match the initial ice concentration in the measurement area (1 m × 0.6 m window) with the concentration obtained in the experiments. No water flow was assumed in the numerical model, while the wind velocity varied along the laboratory channel, following the mean wind speed measured with the PIV system.

Wind plays a crucial role in the formation, movement, and breakup of ice in both rivers and seas. Wu (1968) conducted laboratory experiments that included wind profile surveys, drift current measurements, and water surface observations across a wide range of wind velocities. These experiments were carried out in a wind-wave tank, where various wind profiles were systematically measured. A Pitot-static tube was used to record vertical movements, while

wave height and slope were measured using specialized probes. The boundary layer analysis confirmed a logarithmic velocity distribution, validating the constants used in the model (Wu, 1968). The velocity profile, described by the Kármán-Prandtl velocity distribution, is presented in Equations (1) and (2) (Wu, 1973a).

$$\frac{u_a}{(u_*)_a} = \frac{1}{\mathrm{K}}\ln\left(\frac{y}{k}\right) + 8.5 \quad (1)$$

$$(u_*)_a = \sqrt{\frac{\tau_0}{\rho_a}} \quad (2)$$

In Equation (1), u_a is the measured wind velocity at an elevation of y above the mean surface of water. $(u_*)_a$ is a shear velocity of the wind, K is Karman universal constant equal to 0.4 and k is the roughness depth of the disturbed water under the wind influence. In Equation (1), τ_0 is the wind stress on the water surface, ρ_a is the air density. Based on the logarithmic distribution of Equation (2), wind drag-coefficient (C_y) can be defined by Equation (3) (Wu, 1973b):

$$C_y = \frac{\tau_0}{\rho_a U^2{}_y} = \left[\frac{K}{ln\left(\frac{y}{d}\right)}\right]^2 \quad (3)$$

In which, U_y represents wind velocity measured at an anemometer height of y, above the mean surface of water. $d = \frac{k}{30}$ and denotes the dynamic roughness of water surface disturbed by wind. Wu (1973) provided the values for wind-stress coefficient between 6×10^{-3} to 2×10^{-2} (Wu, 1973b).

DynaRICE model incorporates wind effects using the formulation presented in (Wu, 1973b), where the wind drag-coefficient is set at 0.0015, as commonly used in the literature (Shen, 2016). The wind-shear stress formulation in the DynaRICE model accounts for wind and water velocities but does not consider ice size and concentration. The surface shear stress (τ_s) formulations used in the DynaRICE model are presented in Equation (4) (Shen et al., 1997).

$$\tau_s{}^{(i-a)} = \rho_a C_a \lceil \overrightarrow{v_i} - \overrightarrow{v_a} \rceil (\overrightarrow{v_i} - \overrightarrow{v_a}) \quad (41)$$

In the above equations, ρ_a represents air density, C_a is the wind drag coefficient on ice, $\overrightarrow{v_a}$ is the wind velocity, and $\overrightarrow{v_i}$ is the ice velocity. The experiment aimed to determine whether assuming a constant wind drag-coefficient coefficient is valid, regardless of ice concentration or fragment size.

The laboratory tests revealed that the coefficient proposed by (Wu, 1973b) varies at low wind speeds (below 1 m/s). However, low wind speeds have minimal impact on ice dynamics, especially for large ice fragments. Consequently, the dynamic effects of the ice on structures or shorelines due to wind under such conditions are negligible and can generally be disregarded.

EXPERIMENTAL RESULTS

The laboratory experiments were conducted using a material resembling ice (PP sheets), with varying concentrations of the material floating on the water surface. Figure 2 shows snapshots taken during the experiment, illustrating the distribution of ice concentration for low and high concentration conditions, as well as an ice cover, where the sheets occupy the entire width of the channel. Table 1lists measured ice drift velocities under different combinations of wind speeds and ice concentrations.

Figure 2. Laboratory model of ice, shown in the images from left to right for low concentration conditions, high concentration conditions, and an ice cover

The results of the laboratory experiments are presented in the form of graphs showing ice velocity as a function of its concentration or plate size. The graphs clearly indicate that the effect of concentration is minimal, whereas the impact of the surface area exposed to wind (i.e., plate size) is much more pronounced.

In the extreme cases—large surface area combined with significant mass—when exposed to low wind speed (only one fan operating), no ice movement was observed.

The experiments indicate that the effect of wind on free ice drift (for the ice cover) is nearly constant(Table 2). Differences become noticeable when the concentration is high (nearly full surface coverage with ice), leading to strong interactions between ice fragments. In such cases, free ice drift does not occur, and the role of wind in ice accumulation—especially at low wind speeds—becomes insignificant compared to other forces, such as dynamic water interactions and internal forces within the ice accumulation. Figure 3 illustrates how varying wind conditions influence ice drift velocity across different ice concentration levels.

Table 1. Ice drift velocity under variable wind velocity and ice concentration

	Low wind V_w **= 0.51 m/s**	**Medium wind** V_w **= 1.17 m/s**	**High wind** V_w **= 1.50 m/s**
Low-ice concentration	0.027	0.035	0.042
Medium-ice concentration	0.020	0.033	0.039
High-ice concentration	0.020	0.029	0.035

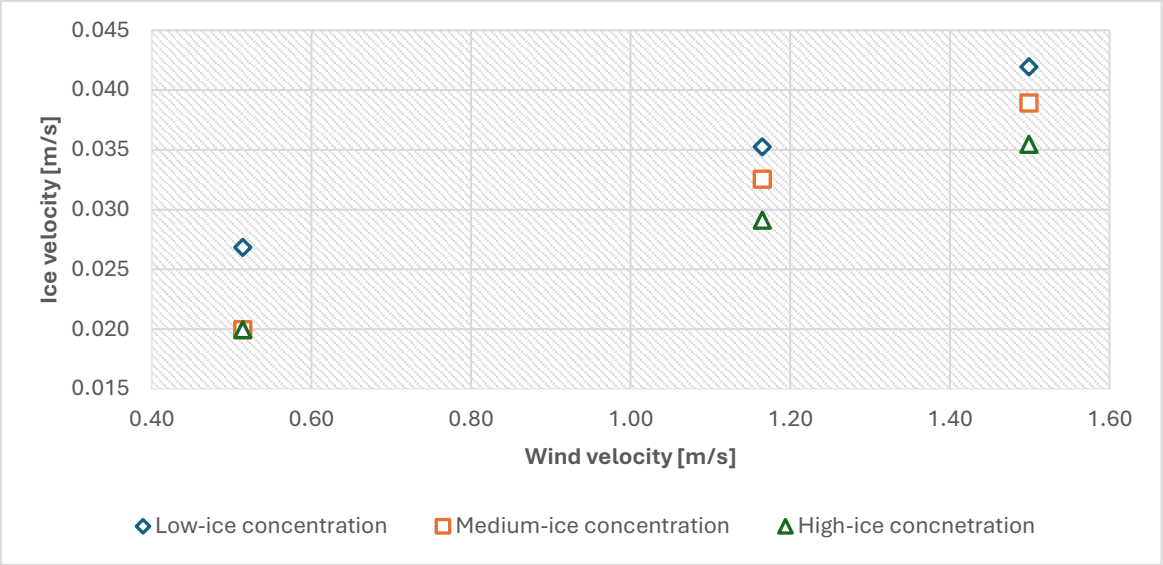

Figure 3. The relationship of wind impact on ice drift velocity under variable ice concentration

Table 2. Ice drift velocity under variable wind velocity for high concentration ice floes and ice cover

Wind velocity [m/s]	Ice velocity [m/s]	
	High concentration ice floes	Ice cover
0,514	0,020	0
1,165	0,028	0,019
1,499	0,035	0,026

Figure 4 shows the correlation between wind forcing and ice drift speed, specifically for high ice concentration and ice cover.

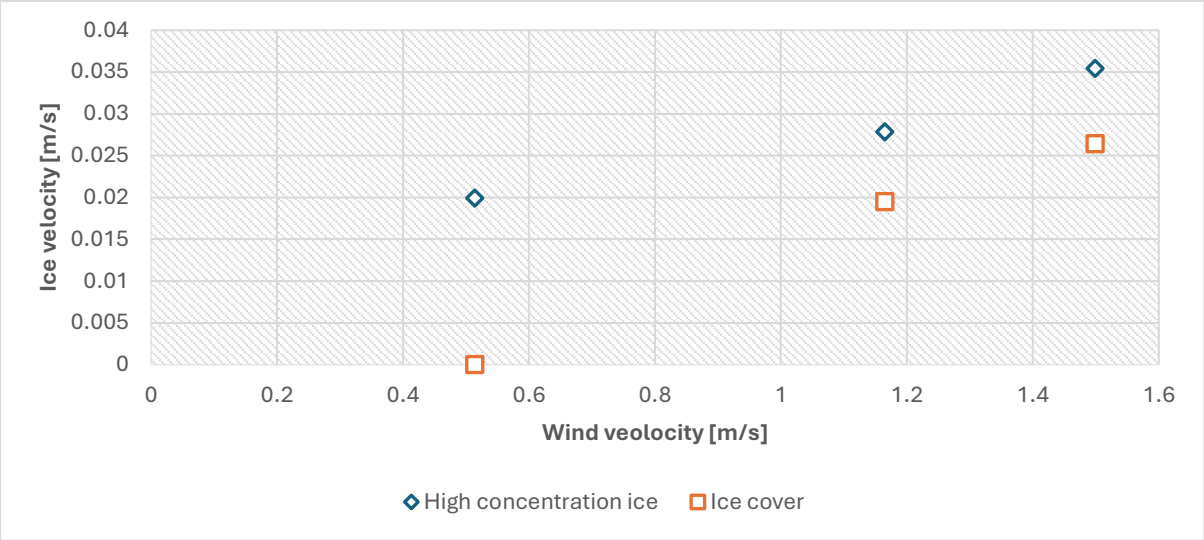

Figure 4. The relationship between wind forcing and ice drift velocity for high-concentration ice floes and ice cover

NUMERICAL SIMULATION RESULTS

The two dimensional mathematical model of the laboratory channel was made for the purpose of the numerical modelling of the ice flow. Numerical simulations were conducted in multiple stages to ensure that the ice concentration on the water surface matched the laboratory experiments. Simultaneously, the experiments had to be conducted in a way that ensured identical wind conditions and hydrodynamics as in the laboratory setup. Figure 5 presents the computational model's domain, including the finite element mesh, with labeled dimensions and identified upstream and downstream boundaries.

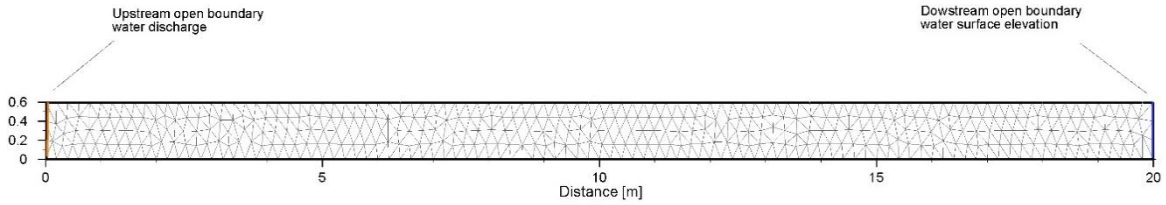

Figure 5. The computational domain with a finite element mesh, presenting the dimensions and the location of the upstream and downstream boundaries

In the first stage, ice was introduced at the upper boundary, along with a steady water flow (constant over time) and a fixed water surface level at the lower boundary. The calculations continued until the ice concentration in the control area (a 1-meter section of the channel) reached the expected value.

The next stage of the numerical experiment involved using the ice concentration obtained in the first stage as the initial condition for further calculations. The initial hydrodynamic condition assumed no water flow in the channel, with a zero-flow upper boundary condition. The wind speed was set according to the direction of flow in the channel, with values identical to the laboratory measurements: 0.51 m/s, 1.17 m/s, and 1.5 m/s. The numerical simulation was

carried out, and the resulting ice velocity was recorded and compared with the values obtained from the laboratory experiments.

For simulations with an ice cover (i.e., measurements for large ice fragments), the numerical simulation followed the methodology for ice motion initiation. This meant that a continuous ice cover was assumed over the entire surface of the laboratory channel. At the start of the simulation, the ice cover was allowed to drift freely, transitioning from a fixed state to motion.

In the mathematical model, this process was implemented by dividing the ice cover into discrete elements that were subjected to both external and internal forces, causing them to move in response to water flow dynamics.

In the numerical experiment, the upper boundary condition assumed zero water flow, while the water surface level was held constant at the lower boundary. The only driving force for ice transport in the experiment was wind, which was applied as a steady force blowing along the channel. The wind speeds were directly transferred from laboratory experiments, with values of 0.51 m/s, 1.17 m/s, and 1.5 m/s.

The numerical simulation results demonstrated a similar trend in ice velocity behavior compared to the recorded displacements on the water surface during the experiments. Due to the differences between simulation results and the observed values end to achieve better agreement of computation results and observed data, additional simulations were conducted, adjusting the interaction coefficient and comparing the results with the measured data. The variability of the coefficient as a function of wind speed was determined and is presented in the table 3.

Table 3. Calibrated values of the wind drag coefficient

	Wind drag coefficient C_a [-]	**Simulated ice velocity V_S [m/s]**	**Experimental ice velocity V_E [m/s]**	**Relative Error $\frac{V_E - V_S}{V_S}$ [%]**
Low wind velocity V_w = 0.51 m/s	0,009	0,029	0,027	-6,52%
Medium wind velocity V_w = 1.17 m/s	0,0025	0,034	0,035	2,72%
High wind velocity V_w = 1.5 m/s	0,002	0,039	0,042	6,71%

SUMMARY AND CONCLUSIONS

The results obtained from the laboratory model confirm that ice drift driven by wind force is inversely proportional to the size of individual ice fragments. For large ice pieces, wind influence on ice movement is minimal or negligible. As ice concentration increases, the free drift of ice particles also decreases the impact of wind on ice dynamics; however, this effect is not significant. In cases of fully ice concentration and accumulation, wind influence becomes marginal.

The default value of the coefficient linking wind speed to ice velocity appears appropriate for wind speeds above 2 m/s. For lower values, nonlinear dependencies related to local air turbulence over the ice surface become more significant, requiring the coefficient to assume values higher than the threshold value of 0.0015.

REFERENCES

Brevis, W., Niño, Y., Jirka, G.H., 2011. Integrating cross-correlation and relaxation algorithms for particle tracking velocimetry. Experiments in Fluids 50, 135–147.

Guest, P.S., Davidson, K.L., 1991. The aerodynamic roughness of different types of sea ice. J. Geophys. Res. 96, 4709–4721. https://doi.org/10.1029/90JC02261

Hammer, T.C., Willems, T., Hendrikse, H., 2023. Dynamic ice loads for offshore wind support structure design. Marine Structures 87, 103335. https://doi.org/10.1016/j.marstruc.2022.103335

Kolerski, T., 2021. Assessment of the ice jam potential on regulated rivers and reservoirs with the use of numerical model results. Cold Regions Science and Technology 191, 103372.

Kolerski, T., Shen, H.T., Kioka, S., 2013. A numerical model study on ice boom in a coastal lake. Journal of Coastal Research 29, 177–186.

Kolerski, T., Zima, P., Szydłowski, M., 2019. Mathematical modeling of ice thrusting on the shore of the Vistula Lagoon (Baltic Sea) and the proposed artificial island.

Liu, L., Shen, H.T., 2005. CRISSP2D Version 1.0 programmer's manual. CEE Report 05–19.Majewski, W., 2011. Ice phenomena on the lower Vistula. Geophysica 47, 57–67.

Overland, J.E., 1985. Atmospheric boundary layer structure and drag coefficients over sea ice. J. Geophys. Res. 90, 9029–9049. https://doi.org/10.1029/JC090iC05p09029

Shen, H.T., 2016. River Ice Processes, in: Wang, L.K., Yang, C.T., Wang, M.-H.S. (Eds.), Advances in Water Resources Management. Springer International Publishing, Cham, pp. 483–530. https://doi.org/10.1007/978-3-319-22924-9_9

Shen, H.T., Lu, S., Crissman, R.D., 1997. Numerical simulation of ice transport over the Lake Erie-Niagara River ice boom. Cold regions science and technology 26, 17–33.

Wu, J., 1973a. Wind-induced turbulent entrainment across a stable density interface. Journal of Fluid Mechanics 61, 275–287.

Wu, J., 1973b. Prediction of near-surface drift currents from wind velocity. Journal of the Hydraulics Division 99, 1291–1302.

Wu, J., 1968. Laboratory studies of wind–wave interactions. Journal of Fluid Mechanics 34, 91–111.